Physical Model Simulation of Shallow Openings in Jointed Rock

Kittitep Fuenkajorn, Chatkun Sakulnitichai and Pongsak Pangpetch

Geomechanics Research Unit, Institute of Engineering, Suranaree University of Technology,

Muang District, Nakhon Ratchasima, Thailand 30000.

Phone (66-44) 224-443, Fax (66-44) 224-448

E-Mail: kittitep@sut.ac.th.

Abstract

Physical model simulations have been performed to determine the effects of depth, joint spacing and orientation on the maximum unsupported span of shallow underground openings under static and dynamic loads. Cubical and rectangular blocks of Phu Phan sandstone are arranged in a vertical test frame to simulate a two-dimensional representation of single rectangular openings in rock mass with two mutually perpendicular joint sets. Results indicate that the normalized maximum span (W/S_V) rapidly increases with the normalized depth (D/S_H), and tends to approach a certain limit for each joint spacing ratio, S_V:S_H. The maximum span increases with decreasing S_V:S_H ratio. Under S_V=S_H condition, increasing the joint angles from 0° to 45° reduces the maximum span by about 20%. At shallow depths the acceleration of 0.225 g can reduce the maximum span by up to 50%. The impact of the dynamic loads however reduces as the depth increases. The test results under both static and dynamic loading compare reasonably well with those calculated from discrete element analyses using the UDEC code.

1. Introduction

Physical test models or scaled-down models have been widely used in the laboratory to simulate the stability conditions of underground openings in rock masses [1-2]. They are commonly used to gain an understanding of the effects of unique rock characteristics, in-situ stress conditions or opening geometries [3]. The simulations usually simplify the actual conditions into two-dimensional problems. Recently some researchers have developed sophisticated devices to allow a three-dimensional simulation for tunnel stability in rock mass under high stresses [4]. As a result failure conditions of the joints and intact rocks around the openings can be simulated simultaneously. Some devices can incorporate the effects of dynamic loading on the rock models [5-6]. The modeling results are often compared with those from numerical simulations, usually by a discrete element analysis, either to verify the predictive capability of the computed results or to confirm the accuracy of the test models [7-8]. Most researchers (e.g. [3, 5]) above concentrate on studying the opening stability under site-specific conditions. Results obtained from the physical test models that can provide a more general solution of the opening stability in rock masses have been rare.

The objective of this research is to perform physical model tests to assess the effects of depth, joint spacing and orientation on the maximum unsupported span of shallow underground openings under static and dynamic loads. The models simulate two-dimensional sections of single rectangular openings in a rock mass with two mutually perpendicular joint sets. The stability under horizontal pseudo-static accelerations of 0.132 g and 0.225 g is investigated. Empirical relations between the observed maximum span, opening depth and joint spacings are derived. They are used to predict the maximum span under shallow depths. The static and dynamic test results are compared with those simulated from discrete element analyses using UDEC code.

RECEIVED 9 January, 2009

ACCEPTED 17 March, 2009

2. Test Platform

The test platform developed by Pangpetch & Fuenkajorn [9] is used in this study (Figure 1). It can accommodate 4 cm thick rock blocks arranged to a maximum depth and width of 1.2 m to simulate a two-dimensional section of shallow openings in a jointed rock mass. A lateral lithostatic pressure is applied on both sides of the model using a column of crystal balls with a diameter of 16 mm packed in the gap between the model and the test frame. Bulk density of the pack of crystal balls is measured as 2.3 g/cc, which is comparable to the density of the intact block of Phu Phan sandstone. Steel grooved rollers mounted underneath the frame are used for testing under dynamic loads. The rollers are placed on a set of steel rails equipped with a high torque motor, gear system and crank arm to induce a cyclic motion to the entire test platform. The frequency and amplitude of the horizontal pseudo-static acceleration can be controlled by adjusting the rotational diameter of the flywheel and speed of the motor.

3. Rock Sample

Sandstone from the Phu Phan formation is used here as rock. It is classified as fine-grained quartz sandstone with highly

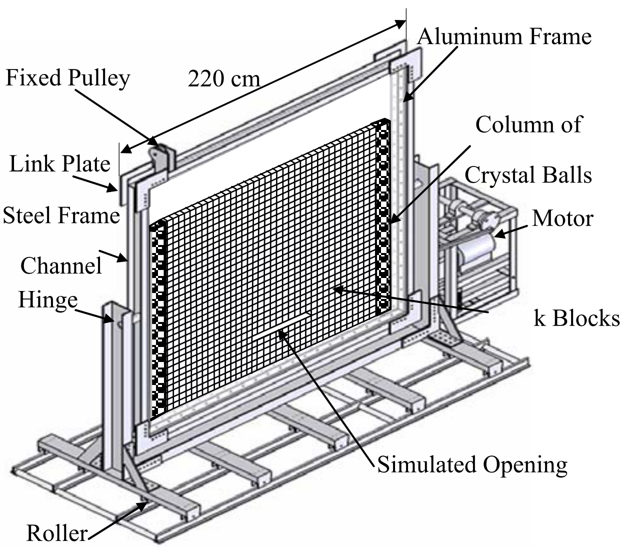

Figure 1 Test platform used to simulate shallow openings in rock mass

uniform texture, density and strength. The average density is 2.27 g/cc. To form rock mass models with two mutually perpendicular joint sets, cubical (4×4×4 cm) and rectangular (4×4×8 cm and 4×4×12 cm) sandstone blocks have been prepared using a saw-cutting machine. The cubical blocks are used to simulate joint sets with equal spacing, while the rectangular blocks simulate joint sets with different spacings. The friction angle and cohesion of the saw-cutting surfaces of the Phu Phan sandstone determined by tilt testing are 26° and 0.053 kPa [9]. The uniaxial compressive strength and elastic modulus of the sandstone determined from related research projects are 62.0 MPa and 10.3 GPa.

4. Test Models under Static Condition

Figure 2 shows the key variables defined in the physical test models. The model height, H, determines the applied maximum lithostatic pressure at the bottom of the model which is calculated as 28.0 kPa. The opening depth, D, is measured from the opening roof to the top of the model. The maximum unsupported span, W, corresponds to the maximum number of rock blocks removed before failure occurs.

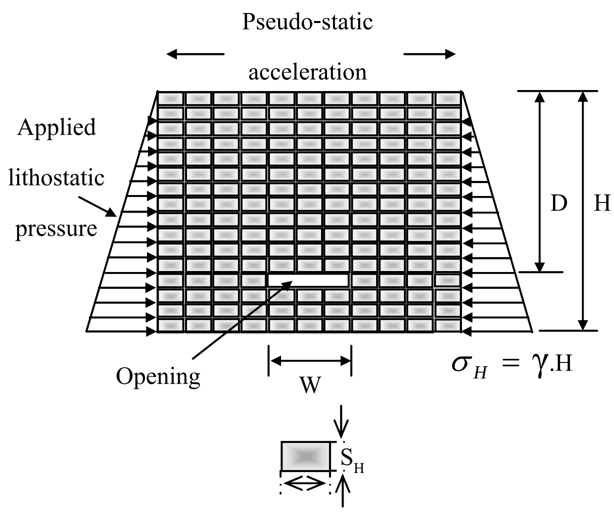

Figure 2 Variables used in physical model simulations and analysis. Joint inclination can be set at any angle by tilting the rock blocks in the model

Spacings for the vertical and horizontal joint sets are defined as S_V and S_H for joint angles of 0° and 90°. For an inclined joint angle the apparent spacings projected on the vertical and horizontal planes are calculated. The effect of opening height is not studied here. It is always set equal to the block height which is the spacing of the horizontal joints, S_H, for each test model. The simulated joint sets have their strike parallel to the opening axis, and hence represent a worst case scenario of the opening stability.

Over fifty test models have been simulated under static condition with S_V:S_H ratios from 1:3, 1:2, 1:1, 2:1 to 3:1. The opening depths vary from 16 to 100 cm. Each set of opening geometries is formed by sandstone blocks with the same dimension. Video records are taken for a post-test analysis. After all blocks are arranged to the maximum height and width in the test frame, a rectangular opening is created by carefully removing a rock block at a pre-defined depth. The blocks adjacent to the opening on both sides are then removed one-by-one until movement or failure of the roof rocks is visually observed. The opening width immediately before the failure occurs is taken as the maximum unsupported span. The test is repeated at least 3 times under the same condition to ensure the repeatability of the results.

Table 1 summarizes the ranges of test parameters and results under static conditions. The observed maximum unsupported spans (W) and their corresponding depths (D) are normalized by spacings of the vertical and horizontal joints (S_V and S_H), respectively. Figure 3 gives examples of the test models for various opening depths and joint spacings. Roof collapse occurs when the opening width exceeds its maximum unsupported span. Figure 4 plots the normalized maximum span (W/S_V) as a function of normalized depth (D/S_H) for various joints spacings. The results indicate that the maximum span increases with depth which can be best represented by a logarithmic equation. As the depth increases, the maximum span approaches an ultimate value

Table 1 Ranges of test parameters and results under static condition

Spacing Ratio (S_V/S_H)	No. of Tests	Depth, D (cm)	D/S_H	Maximum Span, W (cm)	W/S_V
1:1	8	24-92	4.2-16.3	16-40	2.8-7.2
	21	16-96	4-24	12-28	3-7
1:2 or 2:1	8	24-80	4.2-14.1	12-32	2.1-5.6
1:2	12	24-96	3-12	12-28	2-7
1:3 or 3:1	6	28-88	5.1-15.5	12-32	2.1-5.6
1:3	8	24-84	2-7	12-24	3-6
2:1	8	20-92	5-23	8-40	1-5
3:1	8	36-100	9-25	12-48	1-4

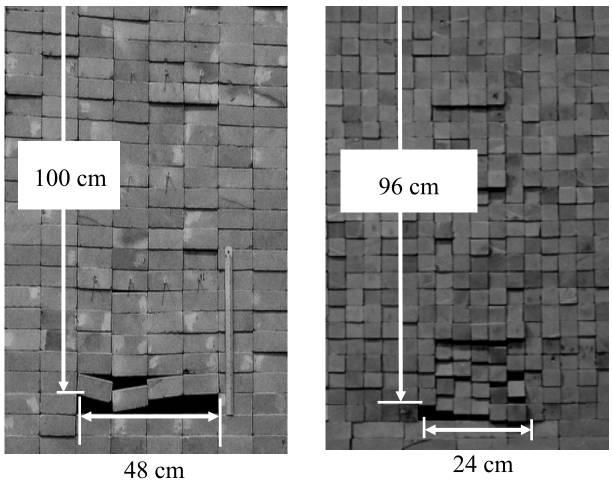

Figure 3 Examples of physical models showing roof failure after opening widths exceed their maximum unsupported spans

for each joint spacing ratio (S_V/S_H). For the condition where S_V=S_H, an inclination of the two joint sets to 45° results in an about 20% decrease in the maximum span.

The empirical relations between the normalized maximum span (W/S_V) and the normalized depth (D/S_H) can be expressed as:

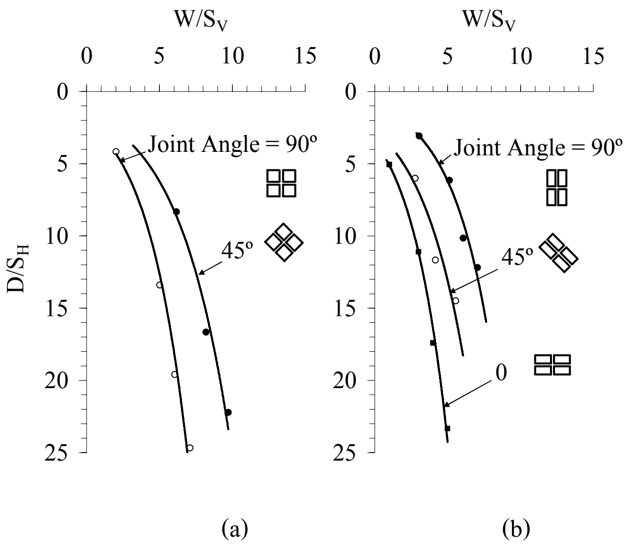

Figure 4 Normalized maximum span (W/S_V) as a function of normalized depth (D/S_H) for various joint spacing ratios and joint orientations

$$W/S_V = A \cdot \ln(D/S_H) - B \quad (1)$$

The constants A and B can be determined as a function of the joint spacing ratio (S_V/S_H) as follows:

$$A = \alpha_A \cdot (S_V/S_H) + \beta_A \quad (2)$$

$$B = \alpha_B \cdot (S_V/S_H) + \beta_B \quad (3)$$

where α_A, β_A, α_B, and β_B are empirical constants. Table 2 summarizes the numerical values for A, α_A, β_A, B, α_B, and β_B calculated for some applicable joint spacing ratios. The empirical relations above can probably represent a lower bound of the maximum unsupported span for actual shallow openings under similar joint conditions and field stresses.

5. Test Models under Dynamic Loads

The effects of the pseudo-static accelerations of 0.132 g and 0.225 g on the maximum unsupported span have been experimentally assessed. Only the horizontal acceleration is simulated here because it has more impact on the geological structures than does the vertical acceleration [10]. The test procedure is similar to that under static condition. Figure 5 plots the normalized maximum span as a function of normalized depth for testing under pseudo-static accelerations of 0.132 g and 0.225 g. Similar to the test results under static condition, the maximum span increases with depth which can be best represented by a logarithmic equation for each joint spacing ratio. Numerical values for the empirical constants are listed in Table 3. As the depth increases, the maximum span approaches an ultimate value. The higher the acceleration applied to the test models, the smaller the maximum span obtained. The acceleration of 0.225 g can reduce the maximum span by up to 50%, particularly when the $S_V:S_H$ ratio is greater than 2:1. As the depth increases the maximum spans under dynamic loads are close to those tested under static condition, suggesting that the impact of dynamic loading decreases with depth. At shallow depth, a pseudo-static force generated by the cyclic motion of the test frame may be high enough to effectively reduce the normal stress at the rock block contacts. This subsequently reduces their shearing resistance, resulting in a relative movement between the rock blocks immediately above the opening. As the depth

Table 2 Empirical relations obtained from regression analysis on the test results under static condition. $W/S_V = A \cdot \ln(D/S_H) - B$, where; $A = \alpha_A \cdot (S_V/S_H) + \beta_A$; $B = \alpha_B \cdot (S_V/S_H) + \beta_B$

Spacing Ratio (S_V/S_H)	Block Arrange-ment	A	α_A	β_A	B	α_B	β_B
1:1		2.76			1.99		
1:2		2.76			0.02		
1:3		1.71	-0.28	2.60	-2.89	1.28	-1.02
2:1		2.56			3.16		
3:1		1.31			1.35		

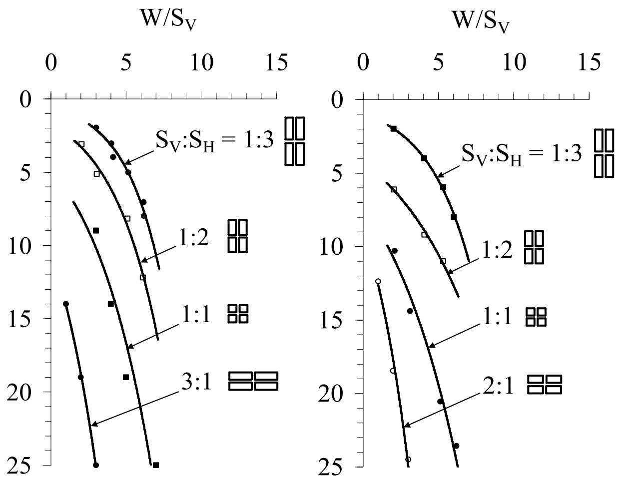

(a) (b)

Figure 5 Normalized maximum span as a function of normalized depth under pseudo-static accelerations of 0.132 g (a) and 0.225 g (b)

Table 3 Empirical relations obtained from regression analysis on the test results under dynamics load at a = 0.132 g and 0.225 g. $W/S_V = A \cdot \ln(D/S_H) - B$, where; $A = \alpha_A \cdot (S_V/S_H) + \beta_A$; $B = \alpha_B \cdot (S_V/S_H) + \beta_B$

a (g)	Spacing Ratio (S_V/S_H)	A	α_A	β_A	B	α_B	β_B
0.132	1:1	3.74	0.24	2.88	5.54	2.95	-0.06
	1:2	3.11			1.65		
	1:3	2.38			-1.28		
	3:1	3.45			8.11		
0.225	1:1	4.93	-0.66	4.69	9.65	2.00	4.06
	1:2	5.49			7.95		
	1:3	2.92			-0.02		
	2:1	2.90			6.34		

increases, the same magnitude of the pseudo-static force may not be high enough to overcome the applied lateral lithostatic stress, and hence have smaller effect on the shearing resistance at the block contacts.

6. Discrete Element Analyses

Discrete element analyses are performed using UDEC code [11] to describe the stability conditions of the openings in the physical models. The discrete element models are constructed to represent various opening depths and joint spacing ratios. The joint friction angle and cohesion used in the simulations are 26° and 0.053 kPa. After several trials (by varying opening widths) the maximum unsupported span can be determined for each opening depth and joint spacing ratio. The UDEC results are compared with those observed from the physical models under static loading in Figure 6 and under dynamic loads in Figure 7 for various S_V:S_H ratios. The UDEC simulations show the increasing trends of the maximum span with depth which are similar to those observed from the test models. For all cases the predicted maximum spans slightly under-estimate the test results. The largest discrepancies are less than 20%. This is probably because the block models in the discrete element analyses are perfectly shaped with identical joint properties while in the test models the block shapes are not perfect and the frictional strength is unlikely to be identical for all contacts (joint surfaces). As a result the rock blocks constructed in the UDEC models can slide easier than those tested in the physical models, and hence yield a slightly narrower maximum unsupported span.

7. Maximum Spans Estimated From Q and RMR Systems

The maximum unsupported span predicted by the empirical equation derived from the test models is compared with those estimated from the RMR and Q systems of rock mass classification [12]. The comparisons are made for an assumed mine opening at depths (D) ranging from 25, 50, 75 to 100 m. The empirical equation derived for the test results of 4×4 cm blocks is used in the comparison. The joint spacings are assumed as 10, 30 and 50 cm. The rating parameters used in the RMR and Q classification systems are determined or

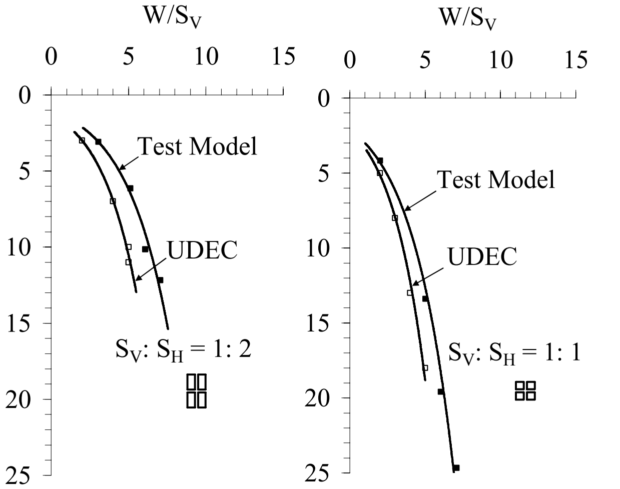

Figure 6 Comparisons of UDEC simulations with test models for various spacing ratios

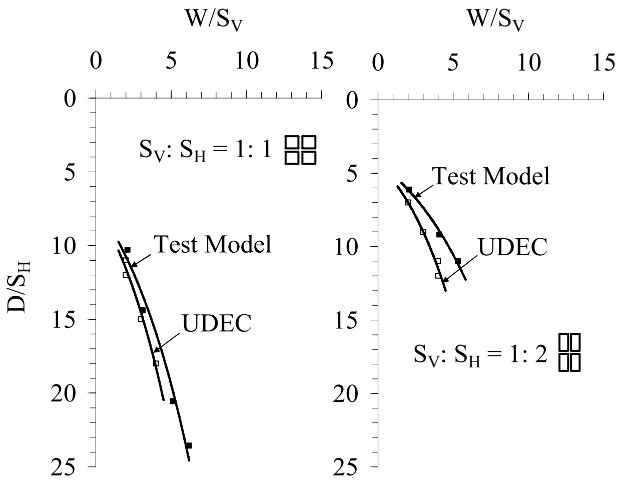

Figure 7 Comparisons of UDEC simulations with test models under pseudo-static acceleration of 0.225 g

projected from the relevant conditions used in the test models.

Table 4 gives the rock mass and joint conditions assumed here. It compares the maximum spans estimated from RMR and Q systems with those predicted from the physical models using empirical equation from Table 2. The physical model predicts the span narrower than the RMR and Q systems do, particularly at shallow depths. This is probably due to the high magnitudes of RQD's estimated from the joint spacings, leading to a high value for RMR and Q, and subsequently makes the calculated maximum span larger. The discrepancies become smaller as the depth increases. At 100 m depth the maximum span from the three methods are comparable.

Under these assumed conditions, the maximum spans determined from the RMR and Q systems are chiefly governed by the joint spacing, and are independent of opening depth. This is because the RMR system does not consider the effect of depth or in-situ stress in the calculation. For the Q system the effect of in-situ stresses is represented by the stress reduction factor (SRF). Here the SRF is set equal to 1.0 because the openings are at relatively shallow depths. The maximum spans predicted by the physical model can however increase with the opening depth and joint spacing, which are probably similar to the actual opening behavior. This is also supported by the UDEC simulation results.

8. Conclusions

The physical model test results clearly indicate that the maximum unsupported span of shallow openings is controlled by the spacing and orientation of joints, S_V:S_H ratio, and depth. The smaller the S_V:S_H ratio, the larger the maximum span. Under the same depth and joint spacing ratio, inclination of the joint angles from 0° to 45° can reduce the maximum span by up to 20%. The tested maximum span increases with depth and approaches an ultimate value for each joint spacing ratio, which conforms to the simulation results from discrete element analyses. The horizontal pseudo-static accelerations of 0.132 g and 0.225 g can significantly reduce the maximum unsupported span for shallow openings. Up to 50% reduction of the maximum opening span resulted for the acceleration of 0.225 g. The effect of the pseudo-static accelerations tends to be more pronounced under a larger S_V:S_H ratio. The dynamic

Table 4 Predictions of maximum unsupported spans using empirical equations and RMR and Q rock mass classification systems

D (m)	Assumed S_V and S_H (m)	RQD	Q	RMR	W from Q system* (m)	W from RMR system** (m)	W from Test model*** (m)
25	0.1	74	0.41	34	5.5	4.5	1.3
	0.3	96	0.53	41	6.1	6.2	3.0
	0.5	98	0.55	51	6.2	9.0	4.4
50	0.1	74	0.41	34	5.5	4.5	1.4
	0.3	96	0.53	41	6.1	6.2	3.5
	0.5	98	0.55	51	6.2	9.0	5.2
75	0.1	74	0.41	34	5.5	4.5	1.5
	0.3	96	0.53	41	6.1	6.2	3.8
	0.5	98	0.55	51	6.2	9.0	5.7
100	0.1	74	0.41	34	5.5	4.5	1.6
	0.3	96	0.53	41	6.1	6.2	4.0
	0.5	98	0.55	51	6.2	9.0	6.0

* For Q system of rock mass classification:

$$W = 2 \cdot ESR \cdot Q^{0.4}$$

ESR = 3.0 (for temporary mine openings), RQD = 100 exp $(-0.1/S_V)(1+0.1/S_V)$, where $S_V = S_H$

$$Q = \left(\frac{RQD}{J_n}\right) \times \left(\frac{J_r}{J_a}\right) \times \left(\frac{J_w}{SRF}\right)$$

J_n = 9.0 (for 3 joint sets), J_r = 0.5 (for slick and planar joints), J_a = 1.0 (for no alteration of joints), J_w = 1.0 (for dry condition), SRF = 5.0 (for loose rock with open discontinuities)

** For RMR system of rock mass classification:
UCS = 62.0 MPa, Open and continuous joints, Correction factor = -12 (for joints with very unfavorable orientation)

*** For physical model (from 4×4 cm blocks): $W = S_V \cdot [2.32 \cdot \ln(D/S_H) - 0.26]$

impact however gradually reduces with depth, as evidenced by the fact that the observed maximum spans under both pseudo-static accelerations are close to those tested under static condition when the normalized depth, D/S_H, approaches 25. Since the models are simulated under very simplified conditions of joints and stress states with a narrow range of test parameters, care should be taken in extrapolating the proposed empirical relations to actual in-situ openings under greater depths or under complex joint conditions and stress states.

9. Acknowledgement

This research is funded by Suranaree University of Technology. Permission to publish this paper is gratefully acknowledged.

References

[1] B. Stimpson, "Simple Physical Modelling Technique for the Demonstration of Interaction between Underground Openings", International Journal of Rock Mechanics and Mining Sciences & Geomechanics Abstracts, Vol.16, No.3, 1979, pp. 217-219.

[2] D.P. Adhikary and A.V. Dyskin, "Modelling the Deformation of Underground Excavation in Layered Rock Masse", International Journal of Rock Mechanics and Mining Sciences, Vol.34, No.3, 1997, pp. 714-719.

[3] W. Zhu and J. Zhao, "Stability Analysis and Modelling of Underground Excavations in Fractured Rocks", Elsevier Geo-Engineering Book Series Volume 1, Series Editor: Hudson, J.A. Netherlands: Elsevier, 2004.

[4] D. Sterpi and A. Cividini, "A Physical and Numerical Investigation on the Stability of Shallow Tunnels in Strain Softening Media", Rock Mechanics and Rock Engineering, Vol.37, No.4, 2004, pp. 277-298.

[5] K. Bakhtar, "Studies under Physical Modeling at 1-g", International Journal of Rock Mechanics and Mining Sciences, Vol.34, No.3-4, 1997, pp. 536.

[6] M. Ma and B.H. Brady, "Analysis of the Dynamic Performance of an Underground Excavation in Jointed Rock under Repeated Seismic Loading", Geotechnical and Geological Engineering, Vol.17, No.1, 1999, pp. 1-20.

[7] R. Bhasin and K. Hoeg, "Numerical Modeling of Block Size Effects and Influence of Joint Properties in Multiply Jointed Rock", Tunnelling and Underground Space Technology, Vol.13, No.2, 1998, pp. 181-188.

[8] H. Zhu, F. Zhang, E.C. Drumm, C.T. Chin and D. Zhang, "2D Model Tests and Numerical Simulation in Shallow Tunneling Considering Existing Building Load", Underground Construction and Ground Movement (GPS 155), Proceedings of Sessions of GeoShanghai 2006, 2006, pp. 304-311.

[9] P. Pangpetch and K. Fuenkajorn, "Simulation of Rock Slope Failure using Physical Model", Proceedings of the First Thailand Symposium on Rock Mechanics, Suranaree University of Technology, Nakhon Ratchasima, 2007, pp. 227-243.

[10] S.L. Kramer, "Geotechnical Earthquake Engineering", Prentice Hall, New Jersey, 1996.

[11] Itasca Consulting Group, Inc., "UDEC 4.0 GUI a Graphical User Interface for UDEC", Minneapolis, Minnesota, 2004.

[12] E. Hoek and E.T. Brown, "Underground Excavations in Rock", The Institution of Mining and Metallurgy, London, 1980.